makeTCR: A Modular Platform for Rapid, Flexible, Scalable, Single-Step T Cell Receptor Synthesis

Authors

M. Hamberger*[1,2,3,4], M-T. Neuhoff*[1,2,3,5], S.V. Pietrantonio[1,2,3,4], T. Boschert[1,2,3], C. Maldonado Torres[1,2,3], A. Errerd[1,2,3,4], C. L. Tan[1,2,3,7], J. M. Lindner[8], M. Platten[1,2,3,4,6,7] and E. W. Green[1,2,3]

1. German Cancer Research Center (DKFZ) Heidelberg, CCU Neuroimmunology and Brain Tumor Immunology, Germany.
2. German Cancer Consortium (DKTK), DKFZ, Core Center Heidelberg, Germany.
3. Department of Neurology, Medical Faculty Mannheim, MCTN, University of Heidelberg, Mannheim, Germany.
4. Faculty of Bioscience, University of Heidelberg, Heidelberg, Germany.
5. Faculty of Engineering Sciences, University of Heidelberg, Heidelberg, Germany.
6. Helmholtz Institute for Translational Oncology Mainz (HI-TRON Mainz), Mainz, Germany.
7. DKFZ-Hector Cancer Institute at the Medical Faculty Mannheim, University of Heidelberg, Germany.
8. BioMed X GmbH, Heidelberg, Germany

* Contributed equally, Correspondence e.green@dkfz-heidelberg.de

Author Contributions (CRediT Taxonomy)

- MH: Methodology, Investigation, Writing – review & editing
- M-TN: Investigation, Methodology, Formal analysis, Writing – original draft, Visualization
- SVP: Methodology, Software
- TB: Methodology, Investigation, Formal analysis, Writing – review & editing
- CMT: Investigation
- AE: Investigation, Visualization
- CLT: Methodology
- JML: Resources, Writing – review & editing
- MP: Funding acquisition, Resources, Supervision, Writing – review & editing
- EWP: Conceptualization, Investigation, Software, Writing – original draft, Writing – review & editing, Project Administration, Supervision, Funding acquisition.

Competing interests

MP, CLT and EWG hold patents and PCT applications describing methods to identify tumor-reactive T cells, and are founders or employees of Tcelltech GmbH. JML is an employee of BioMed X GmbH.

Abstract

Personalised cell therapies utilising T cell receptors (TCRs) show tremendous clinical promise, though TCR synthesis and validation techniques lag behind our ability to sequence TCR repertoires. To address this gap, we developed makeTCR: a flexible modular, scalable TCR cloning system that enables single-step, 100% fidelity assembly of αβ and γδ TCRs into commonly used expression vectors. By implementing cell-free manufacturing, makeTCR enables patient-derived TCRs to be functionally validated within 48 hours. We provide an open-source, easily extensible, web-based graphical platform that integrates existing tools to simplify and standardise the manufacture of TCRs across all scales of synthesis.

Introduction

Human adaptive immunity depends on T cells, which respond to immune challenge by recognising short peptides presented on major histocompatibility complex proteins (pMHC) by means of their unique heterodimeric T cell receptor (TCR). In humans, the process of V(D)J recombination ensures enormous TCR sequence diversity; at any given time a person has around 10^{10} unique TCR clonotypes, allowing for the recognition of a vast range of antigens – including auto antigens in the case of autoimmune disease. TCRs recognising recurrent tumor antigens such as MAGE-A4 [1] or PRAME [2] have been used to genetically engineer autologous T cells to create cellular immunotherapies such as the FDA approved afamitresgene autoleucel. Unfortunately, the costs of identifying TCRs recognising a specific pMHC complex remain high, with the result that most TCR immunotherapies in development target recurrent tumor epitopes presented by the HLA-A*02:01 allele found in about half of Caucasians.

For cancer patients lacking HLA-A*02:01 expression, or whose tumors do not express an antigen targeted by an 'off-the-shelf' TCR therapy, TCRs reactive to patient-specific epitopes can be identified - in some cases resulting in remarkable remissions [3]. Such clinical outcomes raise the hope that personalised autologous TCR T cell therapies may offer clinical benefit for a broad range of patients, however the median vein-to-vein time for creating such a personalised TCR therapy exceeds six months [4]. Recently we and others have shown that the first step of this process – the identification of tumor-reactive TCRs – can be accelerated by identifying these T cells within the TIL population on the basis of single cell sequencing data using gene expression signatures [5–9] or machine learning classifiers [10,11]. However, the manufacture of candidate TCRs remains complex and costly, even when using pre-cloned libraries of TCR V genes with synthetic CDR3-J sequences using either Golden Gate [12] or Gibson assembly [13,14]. Previous TCR cloning approaches were limited by requiring multi-step processes that supported only the manufacture of human αβ TCRs within a single expression vector utilising a single TCR constant region, and also lacked software tools to automate the process of cloning TCRs from TCR repertoire data.

Here we present makeTCR, a modular, Golden Gate-based TCR cloning system that enables single-step, 100% fidelity cloning of both human and mouse, αβ and γδ TCRs into an extensive collection of modular TCR expression vectors and engineered TCR constant domains.

makeTCR's flexibility allows researchers to generate vectors compatible with their existing workflows, whilst benefitting from reduced costs, complexity and turnaround time and increased flexibility. We show that the makeTCR platform can generate entirely novel, patient-derived TCRs in 24 hours, allowing candidate therapeutic TCRs to be validated and prioritised prior to therapy.

To maximise the utility of makeTCR we developed a freely available, open source, graphical web-based companion software platform to automate and simplify the generation of TCRs and HLA-appropriate controls from TCR repertoires and databases that scales from cloning individual TCRs to whole repertoires. Lastly, we show that users can easily propagate hundreds of precloned modules using rolling circle amplification (RCA) in plate-based formats without deleterious effects on TCR assembly fidelity or error rate, improving the useability, cost, and ultimately throughput of TCR synthesis.

88 ## Results

89 **Flexible, high-efficiency modular TCR assembly**

90 We designed a series of mutually orthogonal Golden Gate overlaps to enable BsmBI mediated
91 assembly of αβ and γδ TCRs by combining four pre-cloned modules encoding the germline
92 variable and constant domains of a TCR with a vector backbone and *de novo* synthesised
93 CDR3-TR*J fragments (Figure 1a). By utilising silent codon mutagenesis we generated a set of
94 overlaps between modules predicted to result in 100% fidelity assembly for αβ and γδ TCRs
95 (Figure 1b-d, Supplemental Figure 1). We used these overlaps to split the blue chromoprotein
96 amilCP [15] into six modules, and experimentally confirmed assembly fidelity to be 99.9% using
97 blue/white colony screening in *E.coli* (Supplemental Figure 2a). We used this blue/white
98 assay to rapidly test variant Golden Gate thermocycling protocols, developing an optimised
99 protocol that doubled assembly yield relative to the manufacturer's recommendations
100 (Figure 1e), allowing us to miniaturise TCR assembly reactions without compromising yield.

101 We then generated plasmids encoding the human and murine germline alpha, beta, gamma
102 and delta variable and constant gene sequences flanked by BsmBI recognition sites
103 (Supplemental Table 1). To maximise utility as a 'drop-in' replacement for existing TCR cloning
104 methods we also synthesised a range of commonly used engineered TCR constant regions
105 including variants that limit cross-pairing with endogenously expressed TCRs by incorporating
106 disulfide mutations [16] or switched transmembrane domains [17], variants that increase the
107 amount of surface-expressed TCR by co-expressing CD3z [18], and variants including selection
108 markers mStaygold2 or puromycin N-acetyltransferase to facilitate enrichment or selection
109 of TCR transgenic cells.

110 **A diverse collection of Golden Gate compatible expression vectors**

111 TCRs have been delivered to cells using a panoply of expression vectors including lentivirus,
112 retrovirus, adeno-associated virus (AAV), transposons, and CRISPR/Cas9 mediated knock-in
113 to the genome – typically at the *TRAC* or the *AAVS1* safe harbour loci. We therefore
114 engineered makeTCR compatible versions of each expression vector backbone (Supplemental
115 Figure 3), including homology directed repair (HDR) cassettes that allow for TCR knock-in to
116 the Human *TRAC* locus using either exon targeting [19] or intron targeting guides [20]. In the case
117 of the commonly used pMXS retroviral vector we used structure-guided engineering to
118 deplete BsmBI sites while preserving secondary structure loops in the MMLV Ψ packaging
119 domain. We also created a makeTCR compatible vector containing attL sites, allowing TCRs to
120 be shuttled into existing Gateway™ destination vectors using LR cloning.

121 To ensure high-fidelity cloning of TCRs we engineered all expression vector backbones to
122 incorporate unique SwaI sites to enable vector linearisation (reducing input carryover during
123 vector assembly reactions), and made the vectors cross-compatible with the T-CRAFT high-
124 throughput cloning system by adding appropriate SapI sites [21]. This resulted in a diverse
125 library of Golden Gate compatible vectors supporting high fidelity cloning of TCRs (or other

126 cargoes) to match all commonly used expression vectors, allowing researchers to use
127 makeTCR to complement their existing TCR expression systems.

128 **Simple propagation of cloning modules using rolling circle amplification**

129 One limitation of modular cloning systems is the requirement to maintain large numbers of
130 modules; plasmid DNA preparation from overnight bacterial cultures is a labour- and space-
131 intensive process that is challenging to automate. In contrast, randomly primed, Phi29-
132 mediated rolling circle amplification (RCA) is a simple, cost-effective, high-fidelity method to
133 propagate circular DNA at concentrations similar to a bacterial midiprep using an isothermal
134 reaction that is compatible with plate-based automation [22]. Using our modular amilCP cloning
135 system we could show that assembling amilCP from RCA-amplified input modules resulted in
136 equivalent assembly accuracy (fraction white colonies, P=0.391, Figure 1f,g) and a
137 comparable yield (total number of colonies, P=0.087, Figure 1h) compared to using plasmid
138 encoded modules. We used nanopore sequencing to assess the fidelity of assembled products
139 and detected a small increase in SNPs when using RCA amplified templates (99.18% perfectly
140 aligning reads vs 99.97% using plasmid encoded templates, Figure 1i), confirming previous
141 observations [23]. Given the ease of maintaining module collections by RCA, and the minor
142 increase in sequence error well below the limits of detection for functional TCR validation
143 assays, we performed all further TCR assembly experiments using RCA amplified TR*V and
144 TR*C modules.

145 **Patient-derived TCR prototyping within 48 hours using makeTCR cloning**

146 We previously showed that personalised T cell immunotherapies can be accelerated by using
147 a machine-learning classifier that identifies tumor-reactive TCRs in an antigen-agnostic
148 fashion amongst tumor infiltrating lymphocytes (TILs) using single cell sequencing data [10]. We
149 reasoned that combining rapid TCR identification (predicTCR) and manufacture (makeTCR) to
150 prototype TCRs prior to use in personalised transgenic T cell immunotherapies would likely
151 generate a better TCR product. By using pre-cloned modules makeTCR requires only *de novo*
152 DNA synthesis of the relatively short (<90bp) CDR3a-TRAJ and CDR3b-TRBJ regions; regions
153 that can be generated rapidly in-house using benchtop oligonucleotide synthesisers. We
154 therefore predicted additional tumor-reactive TCRs from our previously described 'BT21'
155 melanoma brain metastasis (Supplemental Table 2) and optimised a cell-free TCR
156 manufacturing strategy that allowed us to generate messenger RNA (mRNA) encoding these
157 TCRs within 24 hours (Figure 2a) – a process that would take over a week using existing
158 approaches. This rapid manufacturing strategy did not reduce overall TCR quality: Nanopore
159 sequencing showed that over 90% of reads for each TCR were free of sequence errors (Figure
160 2b), and transfecting candidate TCR mRNA into TCR-deficient Jurkat cells resulted in high
161 levels of the transgenic TCR in the cell membrane (52.0%-98.1% mTCRb^{+} expression, Figure
162 2c). However, transfection of the same mRNA into healthy donor T cells resulted in a variable,
163 highly repeatable presentation of each TCR ranging from 0.1 % to 32.5% mTCRb^{+} cells (Figure
164 2c). As candidate TCRs were cloned as chimeric TCRs utilising murine constant domains that

165 do not pair with endogenous human constant domains, this likely reflects the differential
166 affinity of each TCR for limited CD3 molecules in the endoplasmic reticulum during maturation
167 [18], with some transgenic TCRs outcompeted by the endogenous TCRs. For three dominantly
168 expressed transgenic TCRs we could confirm reactivity against the BT21 tumor cell line (Figure
169 2d). These results underscore the importance of functionally prototyping TCRs when
170 identifying the best candidates for personalised cell therapy, especially when not ablating the
171 endogenous TCR, and show that such assays can be completed within 48 hours.

172 **makeTCR mediated manufacture of large synthetic TCR libraries**

173 Given the increasing demand for large numbers of synthetic TCRs for both basic and
174 translational research, we developed a variant of makeTCR to support low-cost TCR synthesis
175 using oligonucleotide pools (Figure 3a). We encoded each TCR on a 250 bp oligonucleotide
176 containing the TCR's unique combination of CDR3a-TRAJ and CDR3b-TRBJ sequences
177 bracketed by BsmBI sites, a length-normalizing filler sequence, and a unique pair of mutually
178 orthogonal primers [24](Supplemental Figure 4a,b). This design allows individual TCRs to be
179 amplified from an oligonucleotide pool by PCR, a process that can easily be adapted to 96 or
180 384 well format utilising liquid handling systems. We reasoned that using 96 demultiplexing
181 primers to simplify integration with liquid handling systems allowed for 4,560 unique primer
182 pairs (Figure 3b); at this scale each oligonucleotide can be synthesised for less than €1,
183 resulting in an overall per-TCR manufacturing cost of less than €3.50 (Supplemental Figure
184 4c) – well below the cost of conventional TCR cloning (€80-200).

185 As proof of concept, we manufactured 380 TCRs from our 'BT21' melanoma TIL sample. We
186 adapted the demultiplexing protocol published by Subramanian et al. for use with the high-
187 yield, low-GC bias KAPA HiFi polymerase to minimize primer off-target annealing and ensure
188 selective, high-yield amplification (see Methods). We cleaned and concentration normalised
189 the resulting PCR products using a liquid handling platform, and assembled each TCR with its
190 appropriate V, C and backbone modules using a non-contact dispensing system. We pooled
191 the Golden Gate assembled TCRs, transformed them into *E.coli*, and performed quality
192 control on the resulting plasmid prep. Nanopore long read sequencing revealed a median of
193 80 % of reads resolving to a correctly assembled TCR (Figure 3a), with errors representing
194 both dropouts (missing TCRs) and incorrectly paired CDR3 regions (Figure 3f,g) as a result of
195 imperfect oligonucleotide demultiplexing. Overall, we found that high-throughput arrayed
196 assembly of TCRs using makeTCR resulted in a tight distribution of TCR frequencies suitable
197 for downstream functional screening.

198 **Simple software platform to facilitate TCR manufacture**

199 To simplify and speed the process of cloning and validating TCRs we developed a graphical,
200 web-based tool to automate the process of generating the oligonucleotide sequences
201 required for modular TCR assembly (Figure 4a). The makeTCR software platform accepts
202 diverse input formats, including the Adaptive Immune Receptor Repertoire standard (used by

203 tools such as MiXCR [25]), the **.consensus_annotations.csv* format generated by 10X Genomics'
204 Cell Ranger platform, and the output from VDJdb [26] (Figure 4b). Users can determine which
205 TCRs should be cloned based on TCR frequency, or by submitting a list of target CDR3
206 sequences, with the software internally resolving ambiguous inputs to the IMGT format (e.g.
207 "ASQY" to "CASQYF"). The platform facilitates the cloning of both positive controls (HLA-
208 matched TCRs from VDJdb or MR1-restricted TCRs that have been reported to show broad
209 reactivity against tumor cell lines [27]), and negative controls (randomly selected TCRs from the
210 repertoire). Using the advanced options users can select to clone only TCR within subsets of
211 interest, selecting between αβ, γδ, MAIT or CAIT TCRs (Supplemental Figure 5). Users can
212 then select between the available makeTCR constant regions and expression vectors using
213 annotated dropdown lists, and can easily integrate custom modules in a code-free manner by
214 simply uploading a module's sequence in fasta format. As a fraction of TCRs contain long
215 homopolymer runs in the CDR3 regions that are both difficult to synthesise and accurately
216 sequence (Figure 4d), makeTCR removes these by silent mutagenesis.

217 Once the input parameters are set, the makeTCR software generates vector maps for each
218 TCR (required for QC assemblies), cloning instructions (in both human readable and
219 automation compatible formats), and the DNA sequences that must be ordered for each TCR
220 (Figure 4c). A separate output folder is made for data relating to each method of TCR
221 manufacture; simple synthesis (in which the entire VDJ sequence is exported for users who
222 wish to clone TCRs without access to the pre-cloned modules from makeTCR or TCRAFT), rapid
223 synthesis by oligo annealing, synthesis from arrayed demultiplexed oligonucleotide pools, and
224 the TCRAFT pooled TCR assembly system [21](Figure 4e, Supplemental Figure 6). For arrayed
225 TCR synthesis of more than 383 TCRs we implemented a variant of the two-step nested
226 oligonucleotide demultiplexing strategy of Messemaker and colleagues [28] whereby TCRs are
227 first demultiplexed into pools of 383 using an outer primer pair, and then further
228 demultiplexed in individual wells using a standardised inner pair of primers. This approach
229 allows for a standardised set of 384 primer pairs to be reused for each pool, simplifying setup
230 by allowing replica primer plates to be stamped out. By adding filler DNA sequences to
231 facilitate PCR cleanup, we created an oligonucleotide format that combines simple
232 demultiplexing with flexible TCR assembly.

233 Lastly we extensively documented software options to assist users in selecting the most
234 appropriate format for their TCRs, providing best practice guidelines and linking to the source
235 scientific literature. The software platform is entirely open source, is hosted freely online at
236 https://makeTCR.com, and can be run on private servers as a Docker container when TCR
237 sequences cannot be publicly disclosed.

238 Discussion

239 TCR based immunotherapies are of increasing interest due to the much broader range of
240 targets available to TCRs relative to chimeric antigen receptors (CARs), the decreasing costs
241 of transgenic cell manufacture [29], and the opportunities for developing truly personalised cell

242 therapies [3]. However, the TCR field has not yet coalesced around a rapid, high-fidelity
243 synthesis solution that enables simple, low-cost, flexible yet scalable manufacture of TCRs.
244 We addressed these limitations with the makeTCR platform, which we built to meet the needs
245 of researchers working across different model systems and therapeutic contexts, enabling
246 consistent and reliable TCR assembly of both αβ and γδ TCRs, for both human and mouse
247 sequences. By utilising data-optimized Golden Gate assembly design techniques [30], makeTCR
248 allows for versatile assemblies of VDJ regions grafted onto a TCR constant region of choice
249 without compromising assembly fidelity. Furthermore, makeTCR enables standardized TCR
250 generation regardless of downstream application by providing compatible vectors for all
251 commonly used TCR expression systems; vectors that can be re-utilised for BsmBI mediated
252 cloning of other molecular cargos. For the first time we demonstrate the utility of using Phi29-
253 mediated RCA to substitute for traditional bacterial culture in propagating reusable cloning
254 modules, representing a practical advance that reduces the labour and resources required to
255 maintain a modular plasmid collection while retaining TCR assembly fidelity.

256 A key limitation of previous TCR synthesis techniques was the lack of a software platform to
257 automate the process of generating TCRs from information contained in TCR repertoire
258 datafiles. We developed a free, extensible, open-source graphical platform that allows
259 researchers to upload repertoire sequencing data, select which TCRs they wish to clone, and
260 receive all required DNA sequences, cloning instructions, and vector maps for performing
261 quality control sequencing. By outputting TCR manufacturing solutions for all recently
262 reported synthesis strategies, the makeTCR software platform represents a 'one stop' tool
263 that covers the gamut of TCR manufacture from rapid flexible cloning to high-throughput
264 screening. The software platform is available at https://makeTCR.com, can be run locally (in
265 case of data privacy issues), and can easily be expanded in a code-free manner by users who
266 wish to use novel modules – for example TR*C domains linked to suicide switches enabling
267 the targeted depletion of TCR transgenic cells [31].

268 We have demonstrated that makeTCR enables rapid prototyping of TCRs: novel, patient-
269 derived, tumor-reactive TCRs could be identified, manufactured and functionally validated
270 within 48 hours – a process that previously took multiple weeks [32]. This illustrates the
271 potential of this approach for prioritising patient-derived TCRs with optimal properties such
272 as dominant membrane expression for personalised clinical applications. Our results are
273 particularly timely given the recent FDA 'Fast Track' designation for mRNA encoded TCRs as a
274 monotherapy for HBV-related hepatocellular carcinoma (NCT05195294). This suggests that
275 pipelines combining makeTCR's rapid TCR assembly with cell-free, GMP grade, endotoxin-free
276 manufacture of mRNA, DNA doggybones [33] or nS/MAR vectors [34] could further accelerate -
277 and thereby reduce the cost of - personalised TCR therapies.

278 We have shown that makeTCR scales to high-throughput TCR manufacturing using arrayed
279 TCR manufacture, and supports the design of oligos for pooled library cloning [21]. These large
280 numbers of TCRs can be leveraged in pooled functional screening applications, for example

using synthetic reporters of T cell activation to uncover CDR3 motifs binding recurrent driver mutations [35]. These screens pave the

way for the generation of large curated datasets that can feed into motif discovery and next generation machine learning algorithms aimed at deciphering TCR antigen specificity and predicting therapeutic TCRs for specific diseases or patient subtypes. To facilitate such studies, and the use of the makeTCR resource by the broader immunology research community, all makeTCR modules and vectors are available from both Addgene and the European Plasmid Repository.

Figures

Figure 1: Modular, high fidelity Golden Gate TCR assembly system using makeTCR

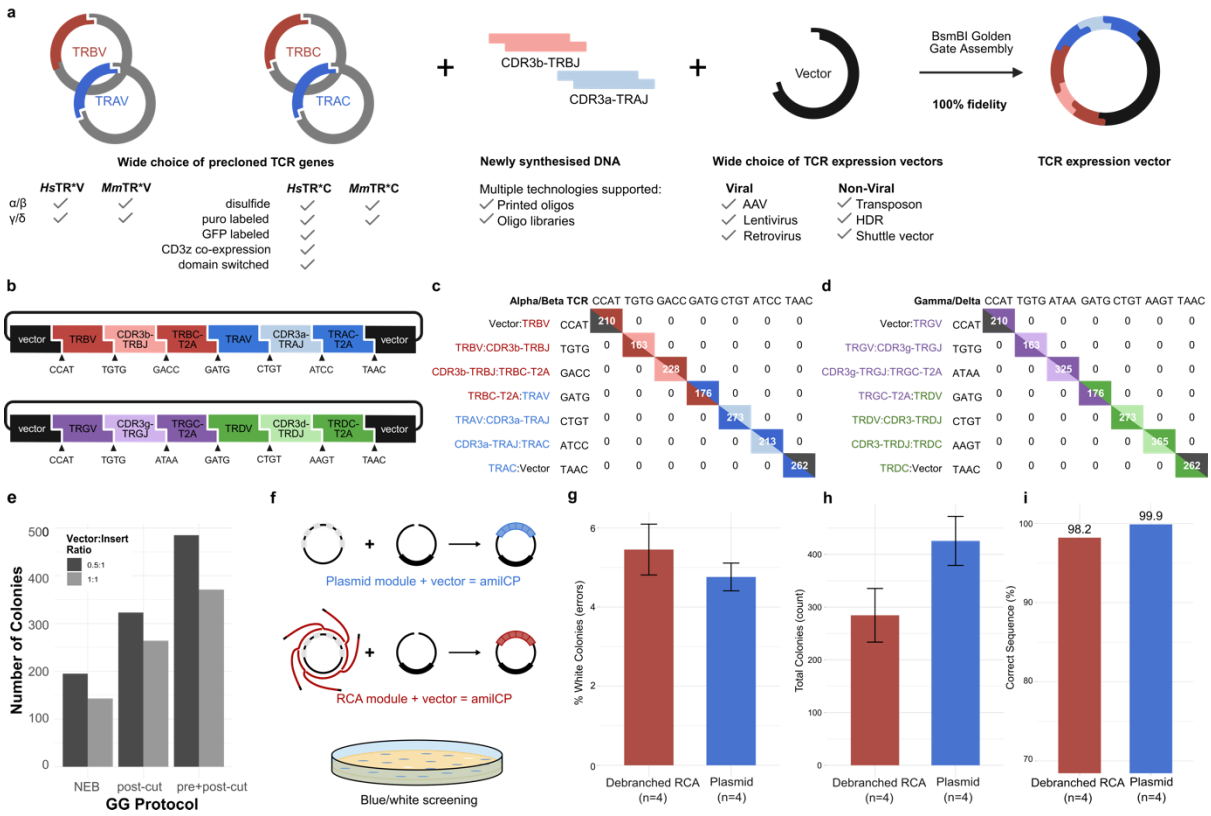

a, Schematic for the makeTCR system of BsmBI mediated modular Golden Gate assembly of TCRs using pre-cloned germline TR*V and TR*C genes, newly synthesised DNA oligonucleotides encoding the CDR3-TR*J regions and a panel of compatible TCR expression vectors.

b, schematic of an assembled polycistronic αβ or γδ TCR expression construct.

c;**d**, ligation fidelity tables showing 100% expected fidelity when assembling αβ or γδ TCRs from makeTCR encoded modules.

300 **e**, modular assembly of the amilCP expression cassettes was used to test variant BsmBI
301 mediated Golden Gate assembly thermocycling protocols; a variant protocol with pre- and
302 post-assembly thermal soak steps resulted in a twofold increase in yield (number of blue
303 colonies).

304 **f**, Experimental setup comparing the efficiency and fidelity of Golden Gate assembly using
305 either plasmid or RCA amplified modules encoding the amilCP chromoprotein

306 **g**, No significant difference in the overall fidelity (number of blue vs white colonies) was found
307 when using plasmid or RCA amplified input (P=0.391, Welch Two Sample t-test, n=4 replicates
308 per template type).

309 **h**, Golden Gate assembly using RCA encoded modules resulted in a non-significant drop in
310 yield vs using plasmid encoded modules (P=0.087, Welch Two Sample t-test, n=4 replicates
311 per condition.

312 **i**, Nanopore sequencing of completed Golden Gate assembly reaction product shows that RCA
313 amplified plasmids exhibit a minor increase in number of SNPs (99.97% perfect reads vs
314 98.18% respectively).

Figure 2: Rapid makeTCR mediated TCR Assembly and TCR Prototyping

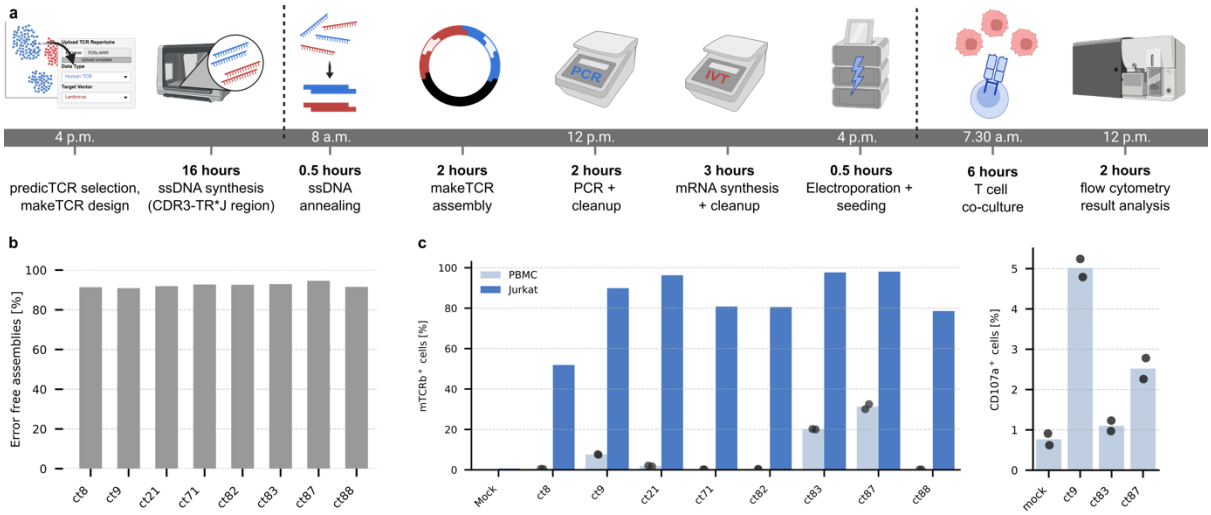

a, Schematic diagram of rapid, cell-free TCR manufacture and testing using an on-site enzymatic oligonucleotide synthesizer and makeTCR modules to generate a polycistronic mRNA for electroporation into T cells.

b, Nanopore sequencing of eight TCR clonotypes from BT21 TILs generated using the rapid makeTCR synthesis approach showed >90% error free reads.

c, Electroporation of IVT generated chimeric TCR mRNA resulted in generally high expression in TCR deficient Jurkat cells (% cells mTCRb^{+}), with previously tested clonotypes showing similar patterns as in Tan et. al. (weak expression of ct8, strong expression of ct9). Short term expression of the same mRNA in primary PBMCs lead to heterogeneous expression (ranging from 0.1 to 32.5% mTCRb+), as some transgenic TCRs are outcompeted for access to the CD3 pool.

d, Co-culture of transgenic REP T cells with the BT21 tumor cell line confirmed the predicted anti-tumor reactivity of strongly expressed TCR clonotypes ct84 and ct87, as well as the ct9 positive control, as assessed by expression of the early activation marker CD107a.

Figure 3: High-Throughput, Oligo-pool mediated makeTCR Assembly

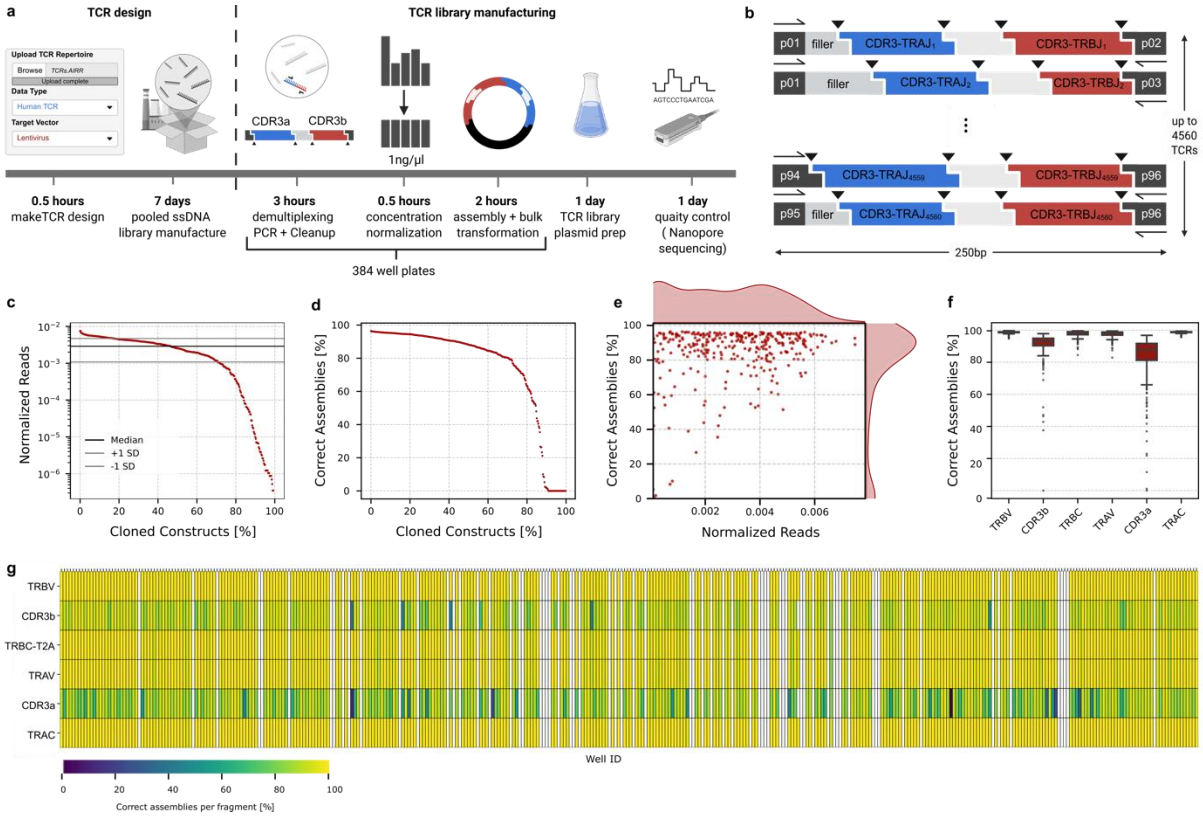

a, Schematic illustrating the use of makeTCR to manufacture TCRs in 384 well plate format by demultiplexing pooled ssDNA oligonucleotides. CDR3a-TRAJ and CDR3b-TRBJ pairs are encoded as 250nt oligonucleotides flanked by a unique pair of mutually orthogonal primer binding sites. Oligos are synthesised in a pooled format, demultiplexed, cleaned and normalised in 384 well plates, before being assembled in miniaturised Golden Gate reactions with appropriate TR*V, TR*C and vector backbone modules. Assembled TCRs are pooled and transformed into *E. coli* to generate a TCR library ready for NGS quality control ready for screening as previously described [36].

b, schematic of oligos format using filler sequences to normalise oligo length to 250 nt. 96 unique primers allow up to 4,560 oligos to be individually amplified from the oligo pool.

c, 380 TIL TCR clonotypes from sample BT21 were synthesised in pooled format, assembled, pooled and Nanopore sequenced to show the distribution of reads mapping to each TCR showing a tight distribution of TCRs with some dropouts.

d, Percentage of error-free TCRs, as assessed number of Nanopore reads having fewer alignment errors than predicted by the Q score of the respective read.

e, combined plot of c and d showing that TCR dropouts are the main cause of error.

f, alignment errors in reads mapped almost entirely to the PCR amplified CDR3 regions (lowest 20 % quantile of TCRs filtered to remove cloned TCRs with insufficient reads for accurate assessment).

352 **g**, Heatmap of 380 TCRs demonstrating correct assembly per fragment on an individual TCR
353 basis.

354 **Figure 4: makeTCR graphical interface**

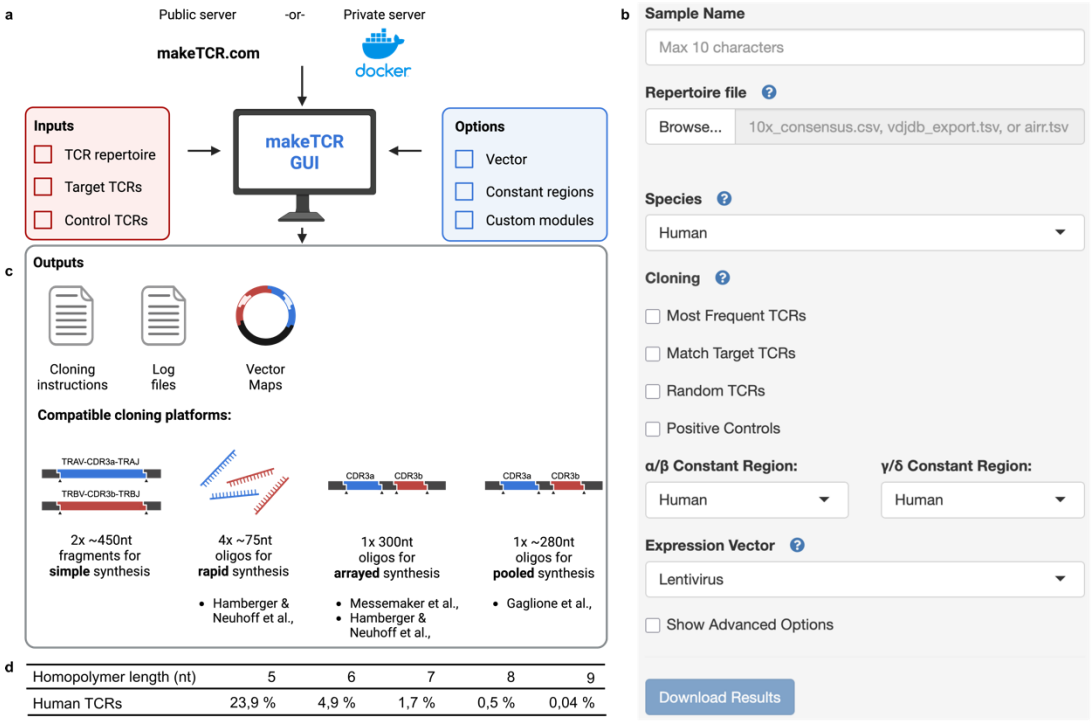

d

Homopolymer length (nt)	5	6	7	8	9
Human TCRs	23,9 %	4,9 %	1,7 %	0,5 %	0,04 %

e

	simple synthesis	rapid synthesis	arrayed synthesis	pooled synthesis
cost/TCR	80 USD	40 USD	3 USD	1 USD
optimal throughput	12-48 TCRs	1-12 TCRs	49-1000 TCRs	>1000 TCRs
robotics needed	no	no	yes	no
time needed	2 days	1 day	2 days	4 days

355

356 **a**, schematic of the makeTCR software platform inputs and outputs.

357 **b**, graphical interface of the makeTCR graphical software platform.

358 **c**, Schematic of outputs provided by makeTCR. Besides log information and vector maps,
359 cloning instructions for a range of cloning workflows are provided.

360 **d**, CDR3-TR*J regions from TCRs derived from a human TIL repertoire natively contain
361 nucleotide homopolymer runs which can be difficult to sequence; makeTCR depletes such
362 homopolymers by silent mutagenesis. Listed are frequency of homopolymers in a human TCR
363 repertoire.

364 **e**, overview and comparison of cloning workflows supported by makeTCR; additional detail of
365 oligo structures shown in Supplemental Figure 6).

Supplementary Information

Supplemental Figure 1: Predicted makeTCR Golden Gate Module Assembly Fidelities

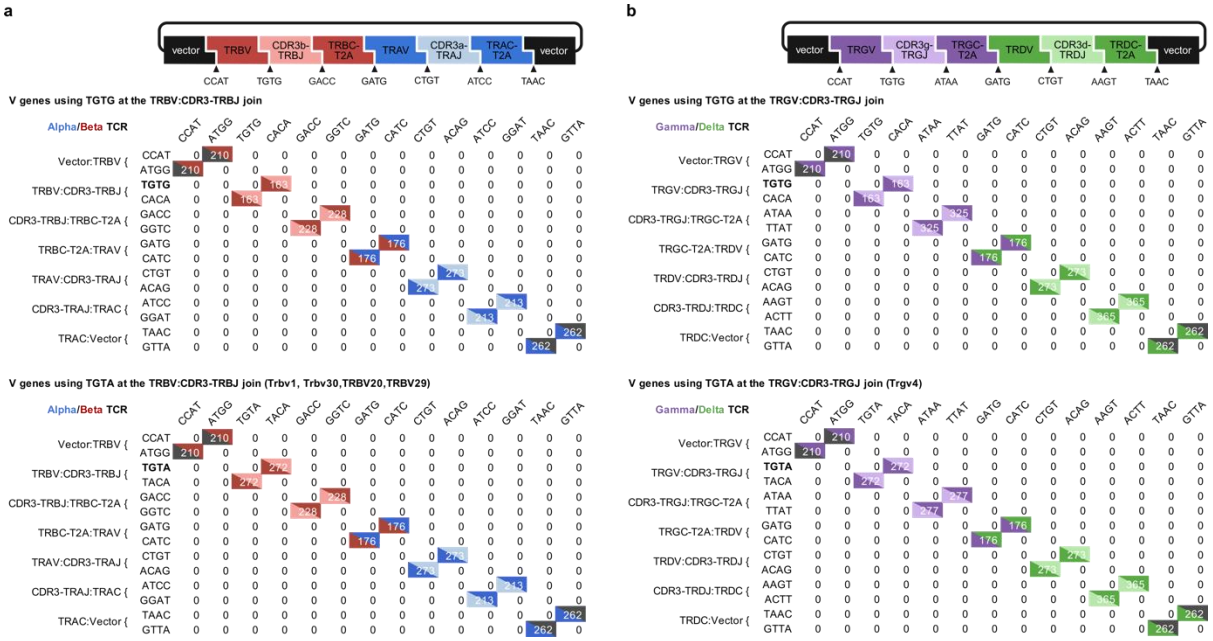

a;**b**, Golden Gate fidelity matrices for cohesive ends linking makeTCR modules for both Alpha/Beta and Gamma/Delta TCRs.

Supplemental Figure 2: Validating assembly fidelity

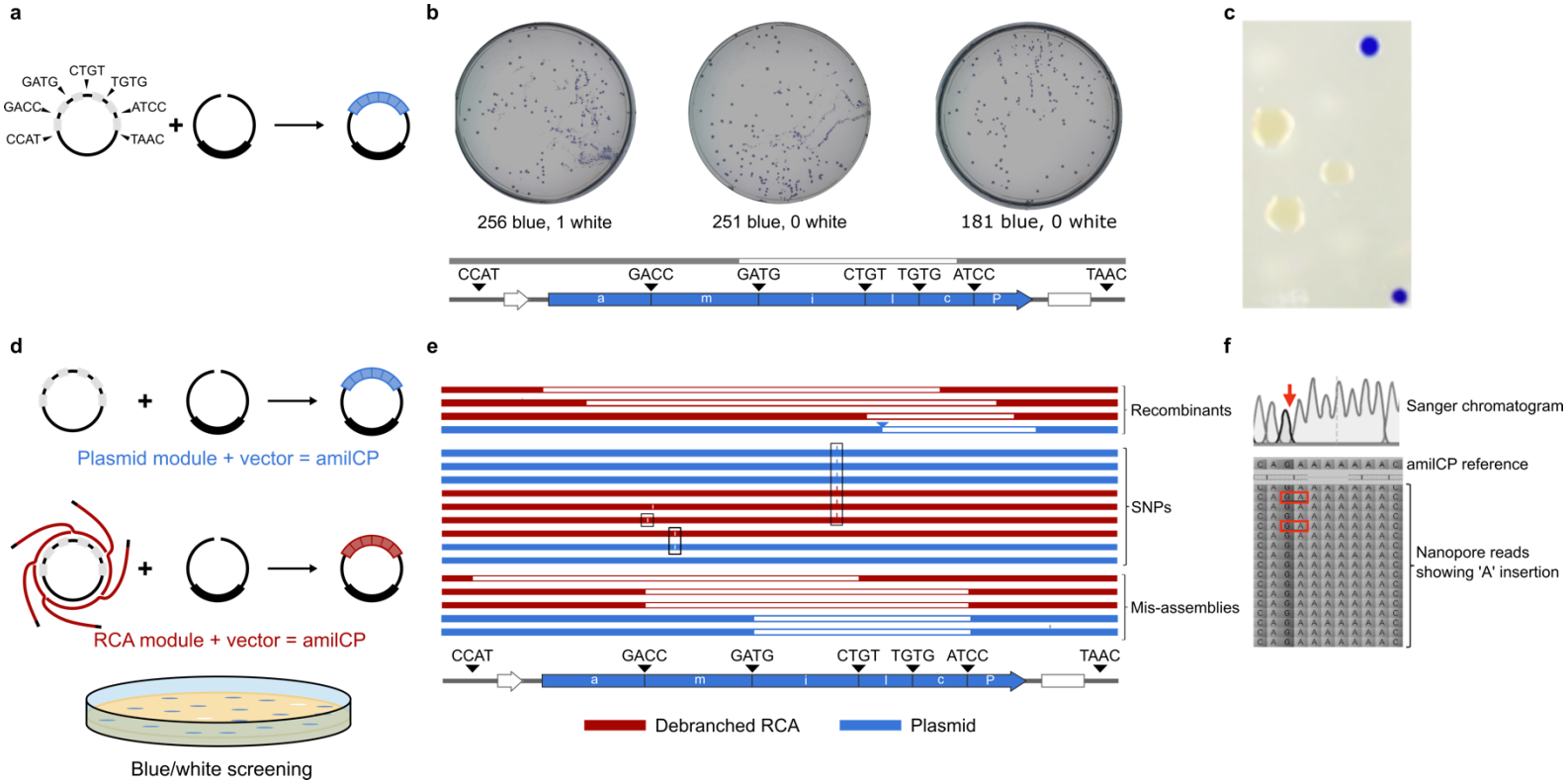

a, A bacterial codon optimised expression cassette encoding the blue chromophore amilCP was split into BsmBI flanked modules linked by the cohesive ends selected to assemble an alpha/beta TCR (CCAT, TGTG, GACC, GATG, CTGT, ATCC, TAAC).

b, The amilCP chromoprotein was assembled in a Golden Gate reaction and used to transform *E. coli*, resulting in 688 blue colonies and 1 white colony: an assembly fidelity of 99.9% vs the computationally predicted fidelity of 100%). The single white colony was Sanger sequenced to show a misassembly event joining the cohesive ends GATG and TGTG, resulting in a truncated non-functional chromophore.

378 **c**, We confirmed previous reports that expression of amilCP from high-copy plasmids imposes at least a 25 % fitness cost on *E. coli* hosts (small
379 blue colonies vs large white colonies)[15]; this ensured that our functional estimates of Golden Gate assembly fidelity were unlikely to be over-
380 estimated due to the selective advantage of loss of amilCP expression in bacteria.

381 **d;e**, Re-assembly of amilCP modules from a plasmid encoded (blue) or RCA amplified (red) template resulted in equivalent numbers of white
382 colonies (Figure 1f-h). We sequenced white colonies assembled from either template types we found equivalent types of errors: amilCP
383 truncation by bacterial recombination (sequence loss not matching module junction sites), Golden Gate mis-assemblies (deletion of regions
384 exactly matching module junction sites), and single nucleotide polymorphisms (SNPs, raised lines representing nucleotide insertions, gaps
385 representing missing nucleotide). We found that in almost all cases SNPs resulted in premature stop codons (black boxes), confirming the
386 selective pressure against amilCP expression (**c**).

387 **f**, We reasoned that SNPs shared between the RCA and plasmid templates must be present in the input plasmid material at levels undetectable
388 by commercial Sanger and Nanopore plasmid QC sequencing. Manual examination of Nanopore plasmid sequencing reads showed that the most
389 common SNP in both assemblies was indeed a rare variant present in the input material.

390 **Supplemental Figure 3: makeTCR expression vectors**

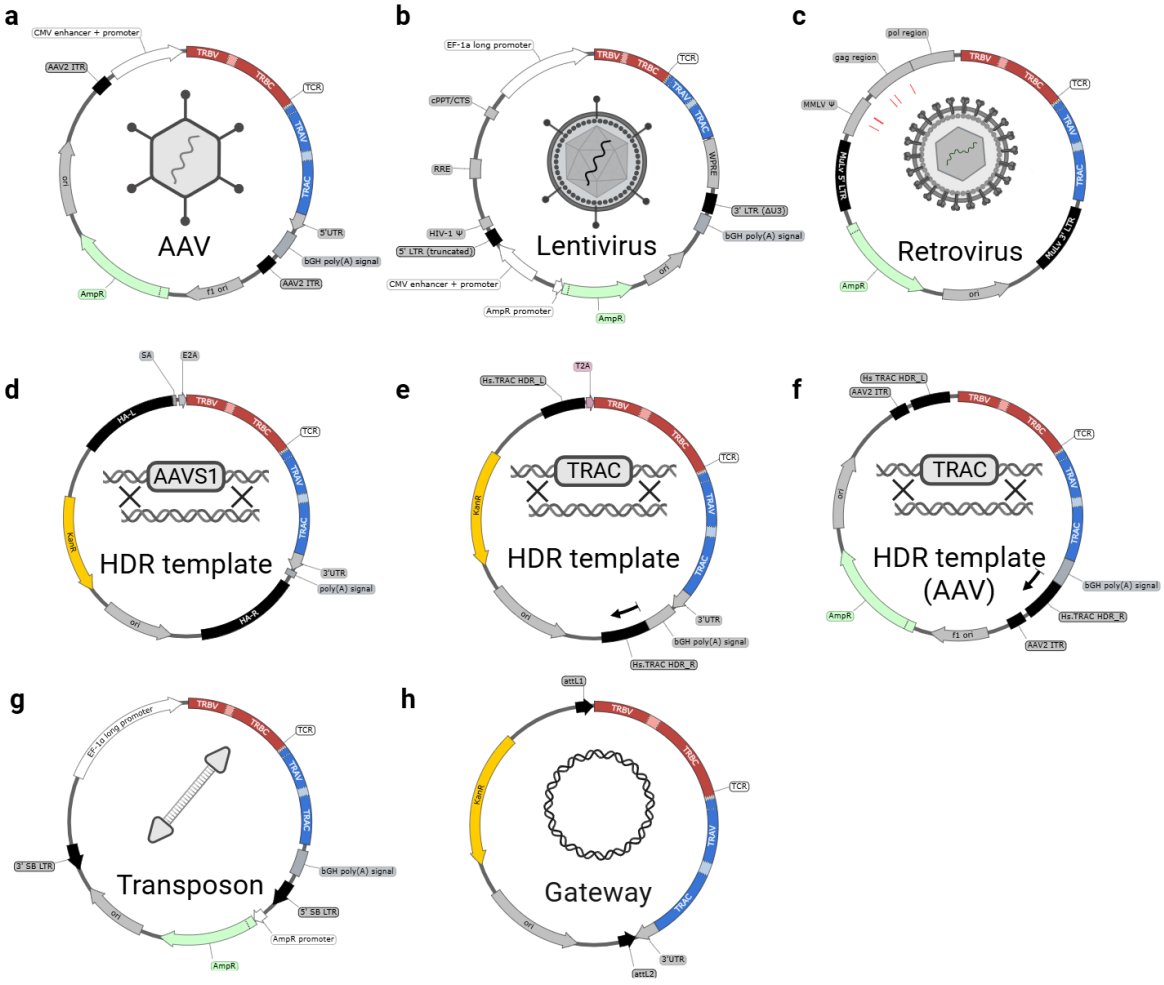

391

392 **a,** AAV vector driving TCR expression using a CMV promoter.

393 **b,** Lentiviral transfer vector driving TCR expression using a long EF1a promoter; truncated LTRs
394 satisfy higher biosafety requirements.

395 **c,** Retroviral TCR expression vector based on pMXS backbone using MMLV LTR region to
396 express TCR.

397 **d,** Vector for HDR mediated integration into the Human genome at the AAVS1; TCR driven by
398 endogenous promoter.

399 **e,** Vector for HDR mediated integration into the Human genome at the TRAC locus; transgenic
400 TCR driven by endogenous TRAC promoter.

401 **f**, AAV2 packaging compatible variant of **e**.

402 **g**, Sleeping Beauty transposon vector; TCR expression driven by long EF1a promoter.

403 **h**, Gateway™ pENTR compatible vector for shuttling TCRs to existing Gateway™ backbones.

Supplemental Figure 4: Example of a high-throughput makeTCR oligonucleotide and pricing breakdown

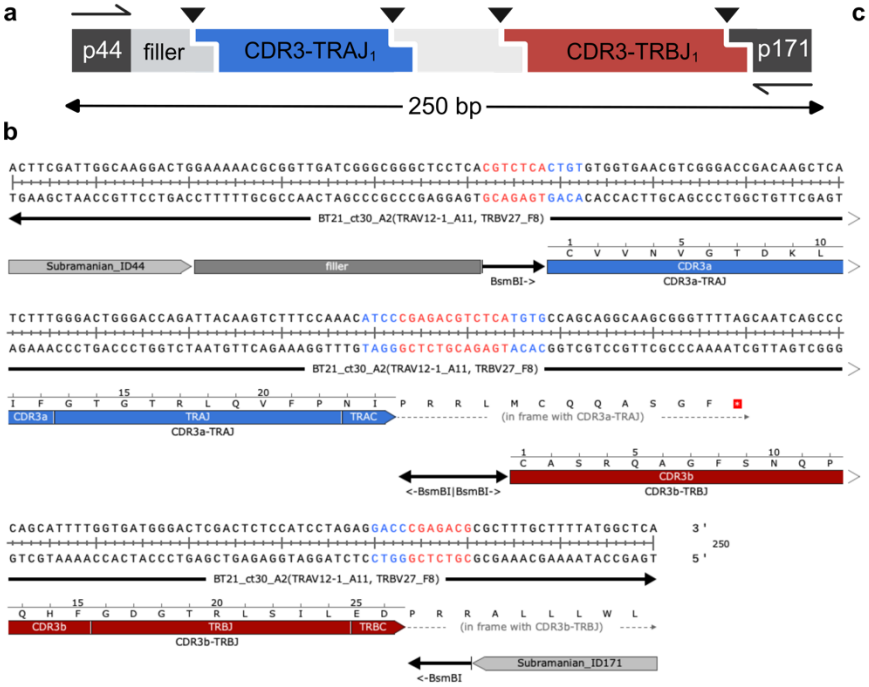

c

Process	Category	Item	2 µl reaction	384 plate
Template	Oligos	250nt ssDNA oligonucleotide	€ 1.00	€ 384.00
PCR	Oligos	Demultiplexing oligos	€ 0.10	€ 38.40
PCR	Plastics	Dispendix S100 primer plates	€ 0.09	€ 35.00
PCR	Enzymes	Kapa Hifi 15µl	€ 0.39	€ 151.20
PCR	Plastics	Twin.tec 384 PCR (0030128532)	€ 0.02	€ 6.80
PCR	Plastics	PCR seal (0030127781) (2x)	€ 0.00	€ 1.36
PCR	Plastics	Integra tips (primer transfer)	€ 0.04	€ 13.80
Cleanup	Beads	Ampure beads	€ 0.12	€ 47.58
Cleanup	Plastics	Agilent Reservoir	€ 0.01	€ 2.40
Cleanup	Plastics	UV Star plate (Greiner 781801)	€ 0.04	€ 15.63
Cleanup	Plastics	Fluotics 70µl filter tips, 6 per well	€ 0.57	€ 219.60
Cleanup	Plastics	PCR seal (0030127781) (1x)	€ 0.00	€ 1.36
Assembly	Plastics	Fluotics 30µl tips	€ 0.08	€ 29.87
Assembly	Plastics	PCR seal (0030127781) (3x)	€ 0.01	€ 4.08
Assembly	Enzymes	BsmBI v2 HF (E1602L)	€ 0.71	€ 270.95
Assembly	Plastics	Twin.tec 384 PCR plate (0030128532)	€ 0.02	€ 6.80
			€ 3.20	**€ 1,228.82**

a, schematic of a 250nt oligo encoding makeTCR compatible CDR3-TRAJ and CDR3-TRBJ regions. **b,** nucleotide sequence of an example oligo sequence (shown as a dsDNA post PCR amplification product, DNA sequence encoding BsmBI sites highlighted in red, cohesive ends for ligation highlighted in blue). **c**, costs of high-throughput makeTCR assemblies when generating 2000 TCRs per manufacturing run.

409 **Supplemental Figure 5: makeTCR platform advanced options**

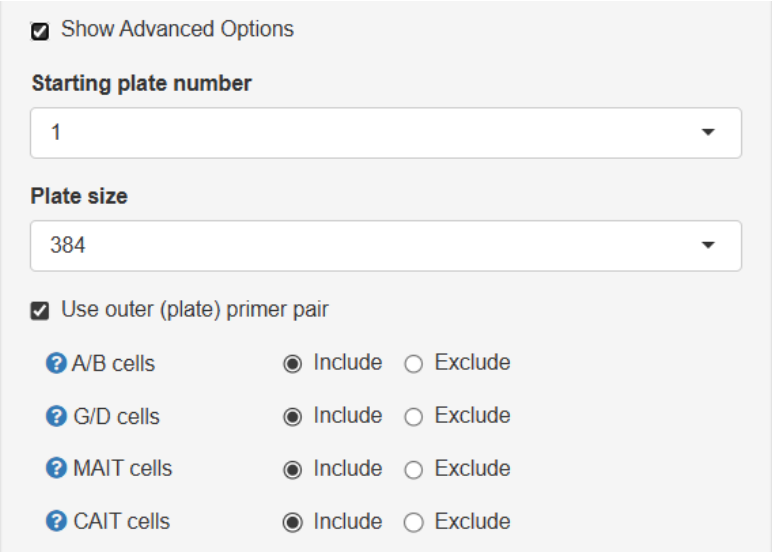

410

411 The makeTCR software platform allows users to select which pair of outer primers (plates 1-
412 8) to append to TCRs, following the schema of Messemaker et al. [28]. If more than 383 TCRs
413 are selected for cloning, primers will be assigned in sequential plate order. Users can also
414 configure whether they have access to 384 or 96 well liquid handlers, which modifies the
415 automation script output and the naming schema for the vector reference maps to make it
416 easy to track which well contains which TCR. Users can also select to only clone certain
417 subtypes of TCR, selecting from αβ, γδ, MAIT and CAIT TCRs.

418 **Supplemental Figure 6: Schematic of TCR cloning oligo formats**

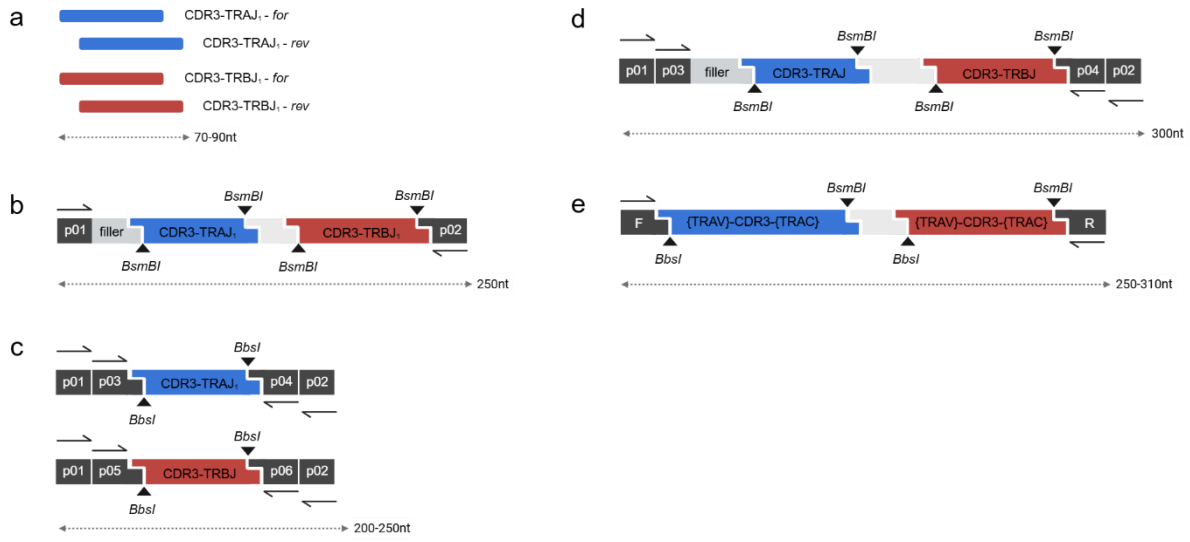

419

420 **a**, makeTCR rapid format: four ssDNA oligos are annealed and used in modular assembly.
421 Strategy requires 4x ~80nt oligos per TCR.

422 **b**, makeTCR arrayed oligo format: each oligo encodes both the alpha and beta CDR3
423 information, and is amplified from a pool using a unique pair of demultiplexing primers. A
424 filler sequencer normalises the length of each oligo. Strategy requires 1x 250nt oligo per TCR.

425 **c**, The original format proposed by Messemaker et al. in which pooled oligos are first amplified
426 as pools using a plate-specific pair of outer enrichment primers (p01 + p02), before being
427 demultiplexed using a well-specific primer pair (p03 + p04 or p05 + p06). Alpha and beta CDR3
428 information is on separate oligos. Strategy requires 2 oligos per TCR, ranging in length from
429 200-250nt.

430 **d**, makeTCR implementation of the Messemaker et al. two round demultiplexing strategy,
431 with the addition of a filler sequence to normalise the length of all oligos. Strategy requires
432 1x 300nt oligo per TCR.

433 **e**, The TCRAFT pooled oligo assembly strategy in which 97% of TCR clonotypes can be encoded
434 on a single oligo (1x 300nt/TCR), and the remaining 3% of long CDR3 TCR clonotypes are
435 ordered as dsDNA fragments.

Supplemental Table 1: makeTCR Germline V Module Sequences

makeTCR modules are distributed on three 96 well plates: 'p2_Hs_V' containing the Human TRAV and TRBV germline modules, 'p 3_Mm_V' containing the Trav and Trbv modules for cloning Murine TCRs, and 'p 4_GD_misc' containing the modules for Human and Mouse gamma/delta TCRs, as well as additional TR*C modules, vectors and uncommonly used Murine germline Trav modules. Addgene_id = Addgene plasmid number, EPR_id = European Plasmid Repository plasmid number *(included as separate file due to table size).*

442 **Supplemental Table 2: BT21 TCR sequences**

443 Sequence of TIL derived TCRs tested in this study from the melanoma brain tumor metastasis sample 'BT21' previously described by Tan et al.
444 [10].. pReactive is the predicTCR calculated probability of a given TCR clonotype being tumor-reactive.

TCR	TRBV	TRBJ	CDR3b	TRAV	TRAJ	CDR3a	pReactive
ct8	TRBV7-3	TRBJ2-1	CASSPGLYNEQFF	TRAV12-2	TRAJ45	CAGYSGGGADGLTF	0.98
ct9	TRBV19	TRBJ2-2	CASSMAGTGGELFF	TRAV27	TRAJ29	CAGESGNTPLVF	0.99
ct21	TRBV5-1	TRBJ2-1	CASSFTSGDSPSSYNEQFF	TRAV8-4	TRAJ6	CAVSSGGSYIPTF	0.94
ct82	TRBV27	TRBJ2-4	CASSYSGSMVKNIQYF	TRAV19	TRAJ52	CALSEAWRAGGTSYGKLTF	0.99
ct83	TRBV9	TRBJ2-1	CASSASGTTSGRGEQFF	TRAV8-6	TRAJ22	CAVTVSGSARQLTF	0.96
ct87	TRBV9	TRBJ2-1	CASSRGNEQFF	TRAV4	TRAJ20	CLVADYKLSF	0.98
ct88	TRBV27	TRBJ2-7	CASSLRTGIEQYF	TRAV17	TRAJ20	CATDAMSNDYKLSF	0.99

445

Material availability

Human germline TRAV and TRBV plasmids, as well as a selection of TR*C plasmids and makeTCR compatible vectors, have been submitted as 96 well plate plasmid collection to Addgene (www.addgene.org) – see Supplemental Table 1, plate '2_Hs_V'.

Murine germline TRAV, TRBV, TRGV and TRDV plasmids, Human TRGV and TRDV, and an extensive collection of TR*C modules and expression vectors are available from the European Plasmid Repository (www.plasmids.eu) – see Supplemental Table 1, plates '3_Mm_V' and '4_GD_Misc'.

Code availability

The makeTCR service is available at https://makeTCR.com, and on publication the source code will be made freely available under MIT license at https://gitlab.com/EdGreen21/makeTCR.

Acknowledgements

- We gratefully acknowledge the data storage service SDS@hd supported by the Ministry of Science, Research and the Arts Baden-Württemberg (MWK) and the German Research Foundation (DFG) through grant INST 35/1503-1 FUGG and INST 35/1503-1 FUGG as well as the German Cancer Research Center Next Generation Sequencing and Flow Cytometry Core Facilities.
- The German Ministry of Education and Science (National Center for Tumor Diseases Heidelberg NCT 3.0 program 'Precision immunotherapy of brain tumors' and the DKTK program) to MP (DKTK equipment grant).
- Federal Ministry of Education and Research (BMBF) and the Ministry of Science Baden-Württemberg, Excellence Strategy of the Federal and State Governments of Germany EMS, flagship 'Engineering Molecular Systems' spotlight proposal 'Synthetic Immunology' and 'Sequencing Oligo Libraries' (ExU 6.1.9).
- Hector Cancer Institute Seed Funding Program to MP, project 445549683,
- M-TN is supported by the Vector Stiftung (P2024-0750).
- CLT is supported by a DKFZ Hector Seed Funding Kick-start EarlyCareer fellowship (C-3PO).
- TB is supported by the Helmholtz-Institute for Translational Oncology Mainz (HI-TRON Mainz) as by a German Cancer Consortium DKTK, DKFZ Joint Funding project award (TRUST) to MP.
- MP received funding from the European Research Council (ERC) under the European Union's Horizon Europe project 101141901.
- We gratefully acknowledge Dr Kim Boonekamp for help preparing figures.
- Figure panels created using BioRender.com.

482 ## STAR Methods

483 **Design and testing of optimal Golden Gate overlaps for TCR assembly**

484 Mutually orthogonal Golden Gate overlaps for assembling TCRs as polycistronic transcripts
485 were iteratively designed to bracket the methionine at the start of TR*V genes, the Cysteine
486 residue defining the CDR3 region, the first complete amino acid of TR*C, and either the end
487 of a T2A linker (for TRBC-T2A and TRGC-T2A) or a TAA encoded stop codon (for TRAC and
488 TRDC) with help of NEB's web based Ligation Fidelity calculator [30] and targeted silent
489 mutagenesis. The final overlaps are shown in Supplemental Figure 1.

490 **Golden Gate assembly fidelity assays using amilCP**

491 We codon optimised the coral *Acropora millepora* chromoprotein amilCP for expression in
492 *E.coli*, splitting the coding sequence into six modules linked by the same Golden Gate overlaps
493 and flanked by BsmBI recognition sites as used to make an αβ TCR (CCAT, TGTG, GACC, GATG,
494 CTGT, ATCC, TAAC). amilCP expression was driven by the constitutive bacterial promoter
495 BBa_J23110 and terminated by the *E. coli* histidine operon terminator. The resulting sequence
496 was ordered as a dsDNA fragment from Twist Biosciences and cloned into a custom backbone.
497 This modular amilCP construct is used as a positive control for makeTCR assemblies; full
498 construct sequence details are available from Addgene (plasmid #233942). The amilCP
499 modular control vector was prepared as miniprepped plasmid, and this was further amplified
500 by RCA and assembled into the makeTCR third generation lentiviral backbone in a BsmBI
501 mediated Golden Gate reaction according to the manufacture's guidelines (plasmid #233943).
502 Assemblies were transformed into NEB stable bacteria, plated on agar and grown overnight
503 at either 30°C or 37°C before allowing the chromoprotein to mature at room temperature
504 (n=4 independent assemblies per condition, 3 technical replicates per assembly).

505 **Manufacture of BsmBI site flanked germline V gene modules**

506 Germline V gene sequences were domesticated by using silent mutagenesis to remove
507 extraneous binding sites for the IIs restriction enzyme BsmBI (CGTCTC) required for TCR
508 assembly using custom R scripts. To ensure maximal downstream compatibility V genes were
509 also optimised to deplete the IIs enzyme BsaI (GGTCTC), the nickase Nt.BbvCI sequence
510 (CCTCAGC), and the rare cutter SmiI/SwaI (ATTTAAAT) to allow for post Golden Gate assembly
511 linearisation of unassembled input material. Sequences were ordered as dsDNA fragments
512 from either Twist Biosciences or Integrated DNA Technologies (IDT) and assembled into the
513 'pMC' custom backbone vector by BsaI mediated Golden Gate assembly. Full vector
514 sequences are available in Supplemental Table 1, as well as from Addgene and the European
515 Plasmid Repository.

516 **RCA mediated amplification of V gene modules**

517 1 ng of each germline V gene plasmid was amplified according to the manufacturer's
518 instructions by randomly primed RCA using New England Biolab's phi29-XT RCA kit in a total
519 volume of 20 µl. Prior to bead purification reactions were diluted 1:5 with nuclease free water
520 to avoid clumping of high molecular weight DNA in the subsequent magnetic bead cleanup
521 (AMPureXP Beckman Coulter). Beads were added to the reaction (0.6X bead to reaction
522 volume) and purification was completed according to the manufacturer's instructions.

523 **Rapid TCR cloning using annealed oligos**

524 Oligos encoding the CDR3-TR*J region were synthesised with a 5' phosphate moiety using a
525 SYNTAX device (DNA Script SAS). Forward and reverse oligos encoding a CDR3-TR*J fragment
526 were annealed in nuclease-free Duplex Buffer (30 mM HEPES, pH 7.5; 100 mM potassium
527 acetate, IDT) in a thermocycler (95°C for 2 min then cooled to 25°C over 25 mins) to generate
528 2 µM annealed dsDNA with cohesive ends compatible with the respective 4 nt makeTCR
529 TRAV/TRAC or TRBV/TRBC assembly sites. Annealed oligos were diluted to 0.2 µM in nuclease-
530 free water and then used in Golden Gate assembly reactions at twice the molar ratio of other
531 components (0.1 pmol of each annealed oligo pair, 0.05 pmol TR*V and TR*C, 0.034 pmol
532 precut vector backbone). Due to the risk of melting annealed oligos, the Golden Gate
533 assembly protocol was modified to include an initial low temperate step (25°C for 20 min),
534 followed by 30 cycles of 42°C/16°C for 1 min each, then an additional 15 min at 42°C, and a
535 final heat inactivation step at 60°C for 5 min.

536 **Generation in vitro-transcribed TCR mRNA constructs**

537 For in vitro transcription, TCRs were assembled into the makeTCR lentiviral backbone which
538 includes an optimised T7 promoter downstream of the elongation factor one alpha (EF1α)
539 promoter used to drive expression in transduced T cells [37]. A linear template for IVT reactions
540 was generated by PCR utilising 0.2 µl of the Golden Gate TCR assembly reaction in a 20 µl
541 reaction using SuperfiII polymerase (Thermo Scientific). 20 cycles of PCR were performed
542 using a Tm of 66°C using the forward primer CAGGTGTCGTGACGTTTAGTG and the reverse
543 primer GGCTGGCACGAAATTGTTG. The resulting PCR product was cleaned using AmpureXP
544 beads (0.6X ratio) and used as a template for the T7 mScript Standard mRNA Production
545 System (CELLSCRIPT C-MSC11610). mRNA was m7G capped and enzymatically polyadenylated
546 following the manufacturer's instructions.

547 **Quality control of TCRs generated from annealed oligos**

548 IVT templates for individually assembled TCRs were prepared as barcoded libraries
549 compatible with Nanopore sequencing using the Native Barcoding kit (SQK-NBD114.24,
550 Oxford Nanopore Technologies). Libraries were sequenced on Flongle flow cell (R10.4.1) on a
551 MinION Mk1D (Oxford Nanopore Technologies) for 24 h. Reads were demultiplexed and
552 basecalled using the Dorado basecaller implemented within MinKNOW, and then aligned to

553 the appropriate TCR reference sequencing using the Clara Parabricks (v4.3.2-1)
554 implementation of Minimap2 (v2.26) [38] . The Dorado basecaller assigns a quality (q-score) to
555 each read; if a read aligned to the reference sequence with fewer mismatches than would be
556 expected from the q-score then that read was called to be error-free.

557 **Isolation and expansion of REP T cells from healthy donor PBMCs**

558 PBMCs from healthy donors were isolated from heparinized blood. 15.5 ml of Ficoll Paque
559 Plus Media (Cytiva) was loaded per Leucosep tube (Greiner Bio-One). After adding 3 ml of PBS
560 (Sigma), up to 25 ml of blood was loaded on top and a density-gradient centrifugation was
561 performed at 800 g. After collection of the interphase, PBMCs were washed twice with PBS
562 and frozen in a controlled rate freezing device at −80 °C in 50 % freezing medium A (60 % X-
563 Vivo 20 and 40 % fetal calf serum) and 50 % medium B (80 % fetal calf serum and 20 %
564 dimethylsulfoxide). Cells were stored in liquid nitrogen at −140 °C until further analysis.

565 The rapid expansion protocol was used to expand T cells. PBMCs from three independent
566 donors were irradiated at 40 Gy using a Gammacell 1000 (AECL) radiation device to serve as
567 feeder cells. Then, 1×10^7 cells from each donor were pooled together, cells were spun down
568 (400 g, 10 min, room temperature) and resuspended in rapid expansion media (X-Vivo15
569 (Lonza, BE02-060Q), 2% human AB serum (H4522-100ML, Sigma-Aldrich), 2.5 µg/ml
570 Fungizone (15290-018, Gibco), 20 µg/ml gentamicin (2475.1, Roth), 100 IU/ml penicillin and
571 100 µg/ml streptomycin (15140122, Life Technologies)). Next, 150,000 PBMCs were plated
572 into a standing T25 flask and 666 ng of OKT-3 antibody (Life Technologies, 16-0037-85) was
573 added to the culture and the flask was topped up to a total volume of 20 ml. The next day,
574 5 ml of X-Vivo15 supplemented with 2 % AB serum containing 7,500 IU interleukin-2 (IL-2) was
575 added to the culture. Three days later, 12.5 ml of medium was removed and replaced with
576 12.5 ml of X-Vivo15 supplemented with 2% AB serum containing 600 IU ml−1 IL-2. We
577 estimated the REP cultures to contain between 40 and 50 % CD8+ T cells using flow cytometry.

578 **TCR reactivity screening via flow cytometry**

579 TCR-encoding RNA was electroporated into expanded healthy donor PBMCs using the Lonza
580 4D-Nucleofector (program EO-115, solution P3 supplemented according to the
581 manufacturer's recommendations). Transfected cells were plated in 48-well plates containing
582 TexMACS media (130-097-196, Miltenyi) supplemented with 2% human AB serum. At 18–24 h
583 after electroporation, cells were collected and 50 IU ml^{-1} benzonase (YCP1200-50KU, Speed
584 BioSystems) was added to avoid cell clumping. TCR expression levels were measured via flow
585 cytometry with markers including fixable viability dye (eFluor 450, eBioscience), CD3 (clone
586 HIT3A, BUV510, BD), and mTCRb (clone H57-597, PE, Biolegend).

587 To assess TCR reactivity, a total of 150,000 T cells and 75,000 cells of the patient-autologous
588 tumor cell line were cocultured in U-bottom 96-well plates in a total volume of 200 µL for 4
589 hours. Wells with only T cells, or T cells and TransAct beads (130-111-160, Miltenyi) were used
590 as negative and positive controls, respectively. Markers included fixable viability dye (eFluor

591 450, 1:1,000 dilution, eBioscience), CD3 (clone UCHT-1, BUV395, 1:100 dilution, BD), CD69
592 (Clone FN50, PE-Cy7, 1:200, Biolegend) and mTCRb (clone H57-597, 1:50 dilution, PE,
593 Biolegend). Samples were acquired on a Biorad ZE5 and flow cytometry data were analyzed
594 using FlowJo software, v10.6.2 (FlowJo LLC).

595 TCRs were classified as reactive or nonreactive based on flow cytometry data acquired after
596 coculture. The percentage of CD69 (%CD69) was quantified by gating on viable $CD3^+$ singlets.
597 TCRs were included in the analysis if the mTCRβ expression was >10%. The CD69 signal per
598 TCR after coculture with the cell line ('TCR versus cell line') or after running the coculture
599 assay without stimulation ('TCR, unstimulated') was corrected for background by calculating

600 (%CD69 TCR vs cellline − %CD69 TCR , unstimulated) − (%CD69 Mock vs cellline − %CD69 Mock,
601 unstimulated)

602 where mock refers to expanded T cells electroporated without TCR-encoding RNA. TCRs were
603 classified as reactive if the background corrected %CD69 signal per TCR was larger than 2×
604 the standard deviation of the %CD69 signal measured in all samples without stimulation.
605 Where a TCR clonotype expressed two α chains, data are presented for the α chain resulting
606 in the higher %CD69 expression (i.e. the functional pair).

607 **ssDNA oligo pool design**

608 Sequences encoding the CDR3a-TRAJ and CDR3b-TRBJ regions for each TCR were modified by
609 silent mutagenesis to remove BsmBI, PaqCI and SwaI restriction enzyme sites. In cases were
610 TCR sequences were to be analysed by nanopore long read sequencing data, homopolymer
611 runs of 6 nucleotides or more were removed by further silent mutagenesis to prevent
612 sequencing artifacts around these regions. BsmBI sites were then appended to the end of
613 each CDR3-TR*J sequence, and filler DNA added to pad all sequences to 210 nucleotides using
614 custom R code to add GC balanced random bases without introducing additional restriction
615 sites, homopolymers, or primer binding sites. Unique pairs of 20nt long primers from
616 Subramanian et al [24] were then added to the ends of the design to make a total of 250
617 nucleotides. An example sequence is shown in Supplemental Figure 4; this strategy allowed
618 for cloning up to a combined total of 61 amino acids for CDR3a-TRAJ and CDR3b-TRBJ.

619 **Library demultiplexing PCR setup**

620 Library demultiplexing was performed in 15 µL reactions using KAPA HiFi HotStart ReadyMix
621 (Roche) with 0.05 ng of single-stranded DNA (ssDNA) oligo pool per well in a 384-well plate
622 format. The demultiplexing PCR mastermix was dispensed into 384-well plates using a
623 microfluidics based non-contact dispenser (Formulatrix Mantis). Two orthogonal primers
624 were dispensed into each well at a final concentration of 0.2 µM, directly from 100 µM 96-
625 well stock plates, using a 96-well plate based non-contact liquid handler (Dispendix I.DOT).
626 We found that cooled PCR setup was essential to prevent KAPA HiFi polymerase's 3'-5'
627 exonuclease activity truncating primers. Following reaction setup, plates were centrifuged at

628 1,000 rcf for 1 min and subjected to orbital shaking on a Bioshake iQ at 3,000 rpm for 3 min.
629 Plates were centrifuged again prior to PCR amplification in an Eppendorf x50t under the
630 following modified conditions: an initial three-step touchdown protocol starting at 65°C was
631 implemented to enhance amplification specificity, followed by 33 cycles of PCR with an
632 annealing temperature of 62°C and an extended annealing time of 40 sec to promote specific
633 priming and efficient on-target amplification despite elevated annealing temperature. We
634 found that using this high primer annealing temperature (relative to the original publication)
635 was key to ensuring specific amplification of target oligos.

636 Post-PCR cleanup was performed using AMPure XP beads, dispensed at a 1:1 bead-to-reaction
637 volume ratio using the Formulatrix Mantis. Plates were then transferred to an Agilent Bravo
638 liquid handling system to perform a magnetic bead-based DNA purification in 384-well
639 format. PCR products were eluted in Greiner UV Star plates and post-cleanup DNA
640 concentrations were measured via absorbance (Varioska LUX Multimode Microplate Reader);
641 custom scripts were then used to normalise all wells to a uniform concentration of 1 ng/µL in
642 deep-well plates.

643 **Golden Gate mediated arrayed assembly of thousands of TCRs**

644 Golden Gate assembly of T cell receptors (TCRs) was performed using the NEBridge® Golden
645 Gate Assembly Kit (BsmBI-v2) following the manufacturer's recommendations, scaled down
646 to a reaction volume of 2 µL. Assembly reactions were prepared in 384-well plates using a
647 Dispendix I.DOT non-contact dispenser to give a ratio of 1 CDR3 oligo : 0.91 TR*V : 0.9 TR*C :
648 0.67 Vector. Corresponding αβ V gene segments, preset constant region modules, and the
649 respective vector of choice were automatically dispensed onto 1 ng of purified oligo DNA per
650 well. Following reagent dispensing, plates were mixed on a Bioshake iQ at 3,000 rpm for 3
651 min and centrifuged at 1,000 rcf for 1 min to collect the reaction. Assembly was performed in
652 an Eppendorf X50t thermal cycler using a custom temperature profile: reactions were
653 incubated at 42°C for 30 min, followed by 30 cycles of 42°C/16°C for 1 min each, then an
654 additional 30 min at 42°C, and a final heat inactivation step at 60°C for 5 min.

655 **TCR library preparation**

656 To generate the pooled plasmid library, 2 µl of each assembled TCR was combined into a
657 single well using an automated liquid handling system (Bravo, Agilent Technologies). Prior to
658 bacterial transformation, the pooled assemblies were purified using AMPure XP beads
659 (Beckman Coulter) at a bead-to-sample ratio of 0.8X to enhance electroporation efficiency.
660 Assembled plasmids were eluted in 60 µl of nuclease-free water and subsequently
661 transformed into electrocompetent *E. coli* (NEB 10-beta, New England Biolabs) following the
662 manufacturer's protocol. To minimize recombination within lentiviral long terminal repeats,
663 bacterial outgrowth was performed at 30 °C for 1 h in NEB's proprietary recovery medium.
664 Cultures were then transferred directly into selective LB medium supplemented with

665 100 µg/mL carbenicillin. To assess transformation efficiency and estimate library coverage,
666 10 µL of the outgrowth was plated on 10 cm LB-agar plates containing the same antibiotic.
667 For all transformations, a minimum of 500X library coverage was maintained. Cultures were
668 expanded at 30 °C for 16–24 h prior to plasmid extraction using a ZymoPURE II Plasmid
669 Maxiprep Kit (Zymo Research).

670 **Nanopore sequencing of TCR libraries**

671 0.01 ng of generated plasmid libraries were used as input for amplicon generation to add UMI
672 adapters to the end of constructs as described by Amstler et al., 2024. UMIs were
673 incorporated by two cyles of PCR (2 min extension at 72°C, 30 s annealing at 60°C) with
674 Platinum SuperFi II PCR Master Mix (Invitrogen) using 0.01 ng of the prepared TCR library and
675 0.5 nM of primers
676 GTCTCTGCTCGACTAACCACTTTVVVVVTVTTVVVVTTVVVTTGTGTGGCTGGCACGAAATTG and
677 GCTCTCATACGAACTCGTCCTTTVVVVVTTVVVTTVVVVTTVVVVTTTAAGTGCAGTAGTCGCCGTG
678 (IDT, machine mixed random bases incl. PAGE-purification. This amplicon was then purified
679 with magnetic beads (Ampure-XP Beckman Coulter, 0.8x ratio). Subsequently, the UMI-
680 tagged product was subjected to a second PCR using Platinum SuperfiII polymerase
681 (Invitrogen) with universal primers binding the last 20 bases of both 5' adaptors of the UMI
682 primers. 0.5 nM of either primer (GCTCTCATACGAACTCGTCC, GTCTCTGCTCGACTAACCAC)
683 was used to amplify the product derived from PCR1 for 25 cycles (annealing 60 °C, 10 s,
684 extension 72 °C 60 s). Nanopore compatible libraries were then generated using either the
685 Ligation sequencing kit (SQK-LSK114) or the Native Barcoding kit (SQK-NBD114.24, Oxford
686 Nanopore Technologies) and sequenced on a PromethION 2 Solo device for three days using
687 a PromethION Flow Cell R10.4.1 or a flongle (R10.4.1) on a Mk1D for 24 h. To reduce compute
688 time we implemented Clara Parabricks (v4.3.2-1) to run Minimap alignments on CUDA
689 GPUs[38]. Secondary and supplementary alignments were subsequently filtered from the
690 generated bam file using samtools [40].

691 **Calculation of correct assembly rate**

692 The assembly rate was calculated as follows: when sequencing pooled, high-throughput
693 manufactured TCRs amplicon reads were first anchored to a TCR reference by filtering for
694 reads containing a perfect alignment to the first and last ten nucleotides of a TCR (thereby
695 depleting reads mapping to residual empty vector that could not be assigned to any one TCR
696 assembly). When sequencing barcoded TCRs generated by rapid TCR assembly this filtering
697 was not required as reads could be mapped to the correct reference TCR by the barcode
698 (derived from the SQK-NBD114.24 kit). Phred scores of the aligned fraction of reads were
699 converted to error probabilities (10^(-Q_score/10); as described by Edgar and Flyvbjerg [41] the
700 expected error rate for each read was characterized by the sum of error probabilities of the
701 alignment region to the reference rounded to the nearest lower integer. The expected error
702 rate was compared to the NM tag of the alignment allowing an estimation of the edit distance
703 between a respective read and its cognate reference (observed errors within the read). Reads

704 with fewer observed errors than expected on the basis of read quality were classified as a
705 perfect assembly; the ratio of perfect assemblies to the number of reads aligning to a
706 particular reference represents the assembly rate.

707 **Assessment of cloning fidelity**

708 When sequencing pooled, high-throughput manufactured TCRs amplicon reads were first
709 aligned against all full-length TCR reference sequences to establish the ground truth TCR for
710 each read. When sequencing barcoded TCRs generated by rapid TCR assembly this filtering
711 was not required as reads could be mapped to the correct reference TCR by the barcode
712 (derived from the SQK-NBD114.24 kit). In both cases reads were then aligned to individual
713 TCR sub-sequences (TRAV, TRBV, CDR3a, CDR3b, TRAC, and TRBC-T2A). Read IDs and their
714 respective reference assignments were extracted from the BAM file, merged, and then
715 compared to evaluate cloning fidelity for each reference. For each individual segment, the
716 percentage of on-target reads aligning to the correct reference was determined (i.e. if a TCR
717 utilised TRBV10-1, what % of reads for this TCR mapped to TRBV10-1).

718

References

1. D'Angelo, S.P., Araujo, D.M., Abdul Razak, A.R., Agulnik, M., Attia, S., Blay, J.Y., Carrasco Garcia, I., Charlson, J.A., Choy, E., Demetri, G.D., et al. (2024). Afamitresgene autoleucel for advanced synovial sarcoma and myxoid round cell liposarcoma (SPEARHEAD-1): an international, open-label, phase 2 trial. The Lancet *403*, 1460–1471. https://doi.org/10.1016/S0140-6736(24)00319-2.

2. Wermke, M., Araurjo, D.M., Chatterjee, M., Tsimberidou, A.M., Holderried, T.A.W., Jazaeri, A.A., Reshef, R., Bokemeyer, C., Alsdorf, W., Wetzko, K., et al. (2025). Autologous T cell therapy for PRAME+ advanced solid tumors in HLA-A*02+ patients: a phase 1 trial. Nat Med. https://doi.org/10.1038/s41591-025-03650-6.

3. Zacharakis, N., Chinnasamy, H., Black, M., Xu, H., Lu, Y.C., Zheng, Z., Pasetto, A., Langhan, M., Shelton, T., Prickett, T., et al. (2018). Immune recognition of somatic mutations leading to complete durable regression in metastatic breast cancer. Nat Med *24*, 724–730. https://doi.org/10.1038/s41591-018-0040-8.

4. Foy, S.P., Jacoby, K., Bota, D.A., Hunter, T., Pan, Z., Stawiski, E., Ma, Y., Lu, W., Peng, S., Wang, C.L., et al. (2023). Non-viral precision T cell receptor replacement for personalized cell therapy. Nature *615*, 687–696. https://doi.org/10.1038/s41586-022-05531-1.

5. Lowery, F.J., Krishna, S., Yossef, R., Parikh, N.B., Chatani, P.D., Zacharakis, N., Parkhurst, M.R., Levin, N., Sindiri, S., Sachs, A., et al. (2022). Molecular signatures of antitumor neoantigen-reactive T cells from metastatic human cancers. Science (1979) *375*, 877–884. https://doi.org/10.1126/science.abl5447.

6. Caushi, J.X., Zhang, J., Ji, Z., Vaghasia, A., Zhang, B., Hsiue, E.H.C., Mog, B.J., Hou, W., Justesen, S., Blosser, R., et al. (2021). Transcriptional programs of neoantigen-specific TIL in anti-PD-1-treated lung cancers (Springer US) https://doi.org/10.1038/s41586-021-03752-4.

7. Zheng, C., Fass, J.N., Shih, Y.P., Gunderson, A.J., Sanjuan Silva, N., Huang, H., Bernard, B.M., Rajamanickam, V., Slagel, J., Bifulco, C.B., et al. (2022). Transcriptomic profiles of neoantigen-reactive T cells in human gastrointestinal cancers. Cancer Cell *40*, 410-423.e7. https://doi.org/10.1016/j.ccell.2022.03.005.

8. Meng, Z., Rodriguez Ehrenfried, A., Tan, C.L., Steffens, L.K., Kehm, H., Zens, S., Lauenstein, C., Paul, A., Schwab, M., Förster, J.D., et al. (2023). Transcriptome-based identification of tumor-reactive and bystander CD8 + T cell receptor clonotypes in human pancreatic cancer . Sci Transl Med *15*, 1–19. https://doi.org/10.1126/scitranslmed.adh9562.

9. Zeng, Z., Zhang, T., Zhang, J., Li, S., Connor, S., Zhang, B., Zhao, Y., Wilson, J., Singh, D., Kulikauskas, R., et al. (2025). A minimal gene set characterizes TIL specific for diverse

tumor antigens across different cancer types. Nat Commun *16*, 1070. https://doi.org/10.1038/s41467-024-55059-3.

10. Tan, C.L., Lindner, K., Boschert, T., Meng, Z., Rodriguez Ehrenfried, A., De Roia, A., Haltenhof, G., Faenza, A., Imperatore, F., Bunse, L., et al. (2024). Prediction of tumor-reactive T cell receptors from scRNA-seq data for personalized T cell therapy. Nat Biotechnol. https://doi.org/10.1038/s41587-024-02161-y.

11. Pétremand, R., Chiffelle, J., Bobisse, S., Perez, M.A.S., Schmidt, J., Arnaud, M., Barras, D., Lozano-Rabella, M., Genolet, R., Sauvage, C., et al. (2024). Identification of clinically relevant T cell receptors for personalized T cell therapy using combinatorial algorithms. Nat Biotechnol. https://doi.org/10.1038/s41587-024-02232-0.

12. Hu, Z., Anandappa, A.J., Sun, J., Kim, J., Leet, D.E., Bozym, D.J., Chen, C., Williams, L., Shukla, S.A., Zhang, W., et al. (2018). A cloning and expression system to probe T cell receptor specificity and assess functional avidity to neoantigens. Blood *132*, blood-2018-04-843763. https://doi.org/10.1182/blood-2018-04-843763.

13. Guo, X. zhi J., Dash, P., Calverley, M., Tomchuck, S., Dallas, M.H., and Thomas, P.G. (2016). Rapid cloning, expression, and functional characterization of paired αβ and γδ T-cell receptor chains from single-cell analysis. Mol Ther Methods Clin Dev *3*, 15054. https://doi.org/10.1038/mtm.2015.54.

14. Zong, S., Mi, T., Flores, L.G., Alpert, A., Olivares, S., Patel, K., Maiti, S., McNamara, G., Cooper, L.J.N., and Torikai, H. (2020). Very rapid cloning, expression and identifying specificity of T-cell receptors for T-cell engineering. PLoS One *15*. https://doi.org/10.1371/journal.pone.0228112.

15. Liljeruhm, J., Funk, S.K., Tietscher, S., Edlund, A.D., Jamal, S., Wistrand-Yuen, P., Dyrhage, K., Gynnå, A., Ivermark, K., Lövgren, J., et al. (2018). Engineering a palette of eukaryotic chromoproteins for bacterial synthetic biology. J Biol Eng *12*, 1–10. https://doi.org/10.1186/s13036-018-0100-0.

16. Cohen, C.J., Li, Y.F., El-Gamil, M., Robbins, P.F., Rosenberg, S.A., and Morgan, R.A. (2007). Enhanced antitumor activity of T cells engineered to express T-cell receptors with a second disulfide bond. Cancer Res *67*, 3898–3903. https://doi.org/10.1158/0008-5472.CAN-06-3986.

17. Bethune, M.T., Gee, M.H., Bunse, M., Lee, M.S., Gschweng, E.H., Pagadala, M.S., Zhou, J., Cheng, D., Heath, J.R., Kohn, D.B., et al. (2016). Domain-swapped t cell receptors improve the safety of TCR gene therapy. Elife *5*, 1–24. https://doi.org/10.7554/eLife.19095.

18. Degirmencay, A., Thomas, S., Holler, A., Burgess, S., Morris, E.C., and Stauss, H.J. (2024). Exploitation of CD3ζ to enhance TCR expression levels and antigen-specific T cell function. Front Immunol *15*. https://doi.org/10.3389/fimmu.2024.1386132.

793 19. Kath, J., Du, W., Pruene, A., Braun, T., Thommandru, B., Turk, R., Sturgeon, M.L.,
794 Kurgan, G.L., Amini, L., Stein, M., et al. (2022). Pharmacological interventions enhance
795 virus-free generation of TRAC-replaced CAR T cells. Mol Ther Methods Clin Dev *25*,
796 311–330. https://doi.org/10.1016/j.omtm.2022.03.018.

797 20. Chang, C.R., Vykunta, V.S., Lee, J.H.J., Li, K., Kochendoerfer, C., Muldoon, J.J., Wang,
798 C.H., Mazumder, T., Sun, Y., Goodman, D.B., et al. (2025). SEED-Selection enables high-
799 efficiency enrichment of primary T cells edited at multiple loci. Nat Biotechnol.
800 https://doi.org/10.1038/s41587-024-02531-6.

801 21. Gaglione, S.A., Mukkamala, R.S., Krishna, C., Smith, B.E., Wadsworth, M.H., Jelinsky,
802 S.A., Perez, C.R., Schmidt-Hong, L., Katz, E.L., Gellatly, K.J., et al. (2025). Scalable TCR
803 synthesis and screening enables antigen reactivity mapping in vitiligo. Preprint,
804 https://doi.org/10.1101/2025.04.24.649726
805 https://doi.org/10.1101/2025.04.24.649726.

806 22. Marano, J.M., Chuong, C., and Weger-Lucarelli, J. (2020). Rolling circle amplification: A
807 high fidelity and efficient alternative to plasmid preparation for the rescue of infectious
808 clones. Virology *551*, 58–63. https://doi.org/10.1016/j.virol.2020.08.016.

809 23. Hejazi, S., Ahsan, A., Kashani, S.M., Tameiv, D., and Reuel, N.F. (2024). Amplified DNA
810 heterogeneity assessment with Oxford Nanopore sequencing applied to cell free
811 expression templates. PLoS One *19*. https://doi.org/10.1371/journal.pone.0305457.

812 24. Subramanian, S.K., Russ, W.P., and Ranganathan, R. (2018). A set of experimentally
813 validated, mutually orthogonal primers for combinatorially specifying genetic
814 components. Synth Biol *3*, 1–5. https://doi.org/10.1093/synbio/ysx008.

815 25. Bolotin, D.A., Poslavsky, S., Mitrophanov, I., Shugay, M., Mamedov, I.Z., Putintseva, E.
816 V, and Chudakov, D.M. (2015). MiXCR: software for comprehensive adaptive immunity
817 profiling. Nat Methods *12*, 380–381. https://doi.org/10.1038/nmeth.3364.

818 26. Shugay, M., Bagaev, D. V., Zvyagin, I. V., Vroomans, R.M., Crawford, J.C., Dolton, G.,
819 Komech, E.A., Sycheva, A.L., Koneva, A.E., Egorov, E.S., et al. (2017). VDJdb: a curated
820 database of T-cell receptor sequences with known antigen specificity. Nucleic Acids Res
821 *129*, 170–177. https://doi.org/10.1093/nar/gkx760.

822 27. Crowther, M.D., and Sewell, A.K. (2021). The burgeoning role of MR1-restricted T-cells
823 in infection, cancer and autoimmune disease. Curr Opin Immunol *69*, 10–17.
824 https://doi.org/10.1016/j.coi.2020.12.002.

825 28. Messemaker, M., Kwee, B.P., Moravec, Ž., Álvarez-Salmoral, D., de Paauw, S., Geerligs,
826 J., Voogd, R., Morris, B., Mußmann, M., Winkler, Y., et al. (2025). A functionally
827 validated TCR-pMHC database for TCR specificity model development. 1 2 3.

828 29. Gotti, E., Tettamanti, S., Zaninelli, S., Cuofano, C., Cattaneo, I., Rotiroti, M.C., Cribioli,
829 S., Alzani, R., Rambaldi, A., Introna, M., et al. (2022). Optimization of therapeutic T cell

830 expansion in G-Rex device and applicability to large-scale production for clinical use:
831 GMP-compliant polyclonal T cell expansion in G-Rex. Cytotherapy *24*, 334–343.
832 https://doi.org/10.1016/j.jcyt.2021.11.004.

833 30. Pryor, J.M., Potapov, V., Kucera, R.B., Bilotti, K., Cantor, E.J., and Lohman, G.J.S. (2020).
834 Enabling one-pot Golden Gate assemblies of unprecedented complexity using data-
835 optimized assembly design. PLoS One *15*, 1–19.

836 31. Sahillioglu, A.C., and Schumacher, T.N. (2022). Safety switches for adoptive cell
837 therapy. Preprint at Elsevier Ltd, https://doi.org/10.1016/j.coi.2021.07.002
838 https://doi.org/10.1016/j.coi.2021.07.002.

839 32. Afeyan, A.B., Wu, C.J., and Oliveira, G. (2024). Rapid parallel reconstruction and
840 specificity screening of hundreds of T cell receptors. Nat Protoc.
841 https://doi.org/10.1038/s41596-024-01061-4.

842 33. Barreira, M., Kerridge, C., Jorda, S., Olofsson, D., Neumann, A., Horton, H., and Smith-
843 Moore, S. (2023). Enzymatically amplified linear dbDNATM as a rapid and scalable
844 solution to industrial lentiviral vector manufacturing. Gene Ther *30*, 122–131.
845 https://doi.org/10.1038/s41434-022-00343-4.

846 34. Bozza, M., De Roia, A., Correia, M.P., Berger, A., Tuch, A., Schmidt, A., Zörnig, I., Jäger,
847 D., Schmidt, P., and Harbottle, R.P. (2021). A nonviral, nonintegrating DNA nanovector
848 platform for the safe, rapid, and persistent manufacture of recombinant T cells. Sci Adv
849 *7*, eabf1333. https://doi.org/10.1126/sciadv.abf1333.

850 35. Cetin, M., Pinamonti, V., Schmid, T., Boschert, T., Fuentes, A.M., Kromer, K., Lerner, T.,
851 Zhang, J., Herzig, Y., Ehlert, C., et al. (2024). T-FINDER: A highly sensitive, pan-HLA
852 platform for functional T cell receptor and ligand discovery. Sci Adv *10*, 1–12.
853 https://doi.org/10.1126/sciadv.adk3060.

854 36. Moravec, Z., Zhao, Y., Voogd, R., Cook, D.R., Kinrot, S., Capra, B., Yang, H., Raud, B., Ou,
855 J., Xuan, J., et al. (2024). Discovery of tumor-reactive T cell receptors by massively
856 parallel library synthesis and screening. Nat Biotechnol.
857 https://doi.org/10.1038/s41587-024-02210-6.

858 37. Conrad, T., Plumbom, I., Alcobendas, M., Vidal, R., and Sauer, S. (2020). Maximizing
859 transcription of nucleic acids with efficient T7 promoters. Commun Biol *3*, 1–8.
860 https://doi.org/10.1038/s42003-020-01167-x.

861 38. NVIDIA (2019). Clara Parabricks . Preprint.

862 39. Amstler, S., Streiter, G., Pfurtscheller, C., Forer, L., Di Maio, S., Weissensteiner, H.,
863 Paulweber, B., Schönherr, S., Kronenberg, F., and Coassin, S. (2024). Nanopore
864 sequencing with unique molecular identifiers enables accurate mutation analysis and
865 haplotyping in the complex lipoprotein(a) KIV-2 VNTR. Genome Med *16*, 117.
866 https://doi.org/10.1186/s13073-024-01391-8.

867 40. Danecek, P., Bonfield, J.K., Liddle, J., Marshall, J., Ohan, V., Pollard, M.O., Whitwham,
868 A., Keane, T., McCarthy, S.A., and Davies, R.M. (2021). Twelve years of SAMtools and
869 BCFtools. Gigascience *10*. https://doi.org/10.1093/gigascience/giab008.

870 41. Edgar, R.C., and Flyvbjerg, H. (2015). Error filtering, pair assembly and error correction
871 for next-generation sequencing reads. Bioinformatics *31*, 3476–3482.
872 https://doi.org/10.1093/bioinformatics/btv401.

873